ELSEVIER

Journal of Molecular Catalysis A: Chemical 167 (2001) 101–107

JOURNAL OF MOLECULAR CATALYSIS A: CHEMICAL

www.elsevier.com/locate/molcata

Photodecomposition of 2,4-dinitroaniline on Li/TiO_2 and Rb/TiO_2 nanocrystallite sol–gel derived catalysts

T. López [a,*], J. Hernandez-Ventura [a], R. Gómez [a], F. Tzompantzi [b], E. Sánchez [b], X. Bokhimi [c], A. García [d]

[a] *Department of Chemistry, Universidad Autónoma Metropolitana-Iztapalapa, P.O.B. 55.534, México 09340 D.F., Mexico*

[b] *Instituto Tecnológico de Ecatepéc, México, Mexico*

[c] *UNAM Instituto de Física, A.P. 20-364, México 01000 D.F., Mexico*

[d] *UPIICSA, COFAA, Instituto Politécnico Nacional, Te No 950, México 08400 D.F., Mexico*

Received 23 May 2000

Abstract

Sol–gel titania was prepared and doped with lithium and rubidium. In samples annealed at 400°C specific surface areas around $100\,m^2/g$ were obtained. By increasing the thermal treatment (600°C) the solids notably diminishes their specific surface area (lower than $27\,m^2/g$). The band gap of the samples was determined by UV–VIS absorption spectroscopy. A decrease of the E_g was observed in titania and doped titania while the temperature was increased. The XRD spectra of the samples showed that at 600°C the main phase in TiO_2 and Rb/TiO_2 was anatase, while in Li/TiO_2 the main phase was rutile. Activities for the 2,4-dinitroaniline photodecomposition suggest an incorporation of lithium in the titania structure, since it is the catalyst showing the lowest activity.

Keywords: Titania sol–gel catalysts; Li and Rb doped titania; XRD of doped titania; UV–VIS band gap on titania; 2,4-Dinitroaniline decomposition on titania

1. Introduction

Titanium dioxide has attracted much attention due to its promising applications in the environmental photocatalytic degradation of pollutants organic compounds in waste water [1–3]. Concerning TiO_2 its doping with numerous ions like noble metals, transition metals, lead, thallium, manganese or cadmium has been carried out in a large number of papers [4]. The effect of doping is to change the equilibrium concentration of electrons or holes. A new set of energy levels accompany these impurity sites, varying the electrical and optical properties of the solid [5]. Another way of changing the electrical properties of titania is by varying the crystallite size [6,7].

Titania has three different crystalline phases; brookite, anatase and rutile. Titanium atoms occupy sites inside deformed oxygen octahedra. The number of shared edges of these octahedra define the crystalline phases. Three octahedra edges are shared in brookite, four in anatase and two in rutile [8]. Pure titania in large crystallite size is stoichiometric and is not useful in photocatalysis. However, when very small titania crystrallite sizes are prepared, anatase

* Corresponding author. Tel.: +52-5-804-4668; fax: +52-5-804-4666.
E-mail address: tesy@xanum.uam.mx (T. López).

1381-1169/01/$ – see front matter
PII: S1381-1169(00)00496-9

and rutile are Ti deficient. The electrical properties of such materials are interesting for applications in photocatalytic reactions [9].

Nanostructured titania can be prepared using the sol–gel method by means of the hydrolysis of titanium alkoxide [10,11]. The method also allows preparation of doped titania by adding different ions to the gel. In such a way, the doping effect magnifies the effect on the band gap [12–14].

Additionally, it has been recently reported that the addition of ions to titanium alkoxide during gelling stabilizes the anatase or rutile structure. For example, gelling titanium alkoxide with hexachloroplatinic acid stabilizes the anatase phase [15]. On the other hand, if platinum acetylacetonate is used, the rutile phase is stabilized at very low temperature [16].

In the present work we present the results obtained in the preparation by the sol–gel method of TiO_2, Li/TiO_2 and Rb/TiO doped catalysts. The objective is to study the ion effect on the stabilization of the titania phase structure, crystallite size, E_g and photoactivity in the 2,4-dinitroaniline decomposition. The alkaline metal were chosen because of their different atomic ratios, 0.60 Å for Li, 1.48 Å for Rb, compared to Ti (0.68 Å).

2. Experimental

2.1. Catalysts preparation

The sol–gel TiO_2 was prepared by mixing 3.2 mol of deionized distilled water with 1.2 mol of ethanol (Baker 99.9%) and 0.2 ml of nitric acid (Baker 65% in water) to obtain pH 3, the solution was put in reflux at 70°C and stirring constantly. Then, 0.2 mol of titanium *n*-butoxide $Ti(Obut)_4$ (Aldrich 99.9%) was added drop by drop while refluxing to the mixture for 4 h until the gel was formed. This gave a water/alkoxide molar ratio of 16.

The doped Li/TiO_2 and Rb/TiO_2 sol–gel catalysts were prepared following the method described for the TiO_2 sol–gel synthesis, adding in the hydrolysis water the corresponding amount of LiCl or RbCl (Baker 99.9%) to obtain 1.0 wt.% of each one. After gelling the samples were dried at 70°C for 24 h. Thermal treatments were done in air for 12 h at 400 and 600 with a heating rate of 20°C/min.

2.2. Specific surface area determination

The specific surface area of the catalysts was determined by the BET method, starting from the nitrogen adsorption isotherm at 77 K, with a Micromeritics ASAP-2000 apparatus. Mean pore size diameter distribution was calculated from the BET isotherm by applying the BJH method in samples calcined at 400 and 600°C. Before adsorption the samples were desorbed in vacuum at 400°C for 6 h.

2.3. UV–VIS absorption spectra

The UV–VIS absorption spectra of the solids were obtained with a Cary-III spectrophotometer coupled to an integration sphere for diffuse reflectance studies. A sample of MgO 100% reflectance was used as reference.

2.4. X-ray diffraction analysis

X-ray diffraction patterns were measured at room temperature with a Siemens D-500 diffractometer using Cu Kα radiation on specimens prepared by packing sample powder into a glass holder. Intensity was measured by step scanning in the 2θ range between 10 and 110°, with a step of 0.02° and a measuring time of 2 s per point. Diffraction peak profiles were modeled with a pseudo-Voigt function that used the average crystallite size as a fitting parameter [17–19]. The standard deviations are given in parenthesis.

2.5. Catalytic activity

Photolysis experiments were carried out at room temperature. In a flask containing an aqueous solution at 30 ppm of 2,4-dinitroaniline, 100 mg of catalyst were added. Under stirring the solution was irradiated in a closed box with a UV lamp Black-Ray model XX-15L, which emits a radiation $\lambda = 254$ nm and an intensity of 1600 $\mu W/cm^2$. The light intensity received by the vessel was 1560 $\mu W/cm^2$. The reaction rate was followed taking aliquots each 10 min and then analyzed in a UV–VIS spectrophotometer Hewlett-Packard model 8452 equipped with a diode array as detector. The concentration of 2,4-dinitroaniline was calculated from absorption band at 346 nm.

Table 1
Specific surface areas and band gap (E_g) for TiO_2, Li/TiO_2 and Rb/TiO_2 sol–gel catalysts

Sample	(°C)	BET area (m^2/g)	λ (nm)	E_g (eV)
TiO_2	400	111	378	3.27
	600	21	410	3.02
Li/TiO_2	400	89	373	3.32
	600	6	401	3.08
Rb/TiO_2	400	114	378	3.27
	600	3	385	3.21

3. Results and discussion

3.1. Specific surface area, pore volume and pore size distribution

Data of specific surface areas are shown in Table 1, for samples calcined at 400 and 600°C. The samples treated at 400°C show specific surface areas of 117, 95 and115 m^2/g for TiO_2, Li/TiO_2 and Rb/TiO_2, respectively. However, by increasing the thermal treatment at 600°C the BET areas drastically diminishes (21, 6 and 3 m^2/g). These results are indicative that non-important effects of Li or Rb can be observed in the textural properties of the TiO_2.

3.2. UV–VIS spectroscopy

The evaluation of the band gap (E_g) of the samples was calculated in the present work using the equation $\alpha(h\nu) = A(h\nu - E_g)^{m/2}$, were α is the absorption coefficient, $h\nu$ the energy of the photon and $m = 1$ for a direct transition between bands. From the UV–VIS spectra, E_g was calculated by extrapolation of the straight line from the absorption curve to the abscissa [20]. On applying this method we have an accuracy of ±0.01 eV. Experimental UV–VIS spectra of the Rb doped sol–gel titania samples treated at 400°C are shown in Fig. 1. The calculated E_g for the samples is reported in Table 1. It can be seen that in general, there is a decrease of the E_g as the temperature of the thermal treatment increases.

3.3. X-ray diffraction patterns

In order to analyze quantitatively the crystalline phases, XRD patterns were made. The phase

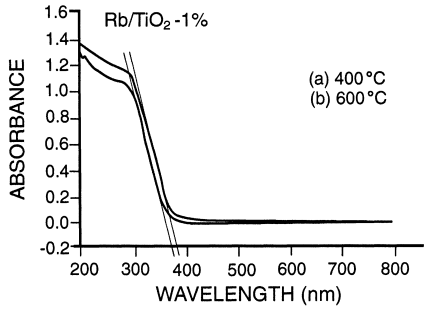

Fig. 1. UV–VIS spectra of Rb/TiO_2 sol–gel catalysts annealed at 400 and 600°C.

Table 2
Titania phase composition as a function of dopant and temperature

Catalyst	(°C)	Anatase (wt.%)	Rutile (wt.%)	Brookite (wt.%)	$LiTiO_2O_4$ (wt.%)
TiO_2	400	94		6 (1)	
	600	88 (2)	12 (1)		
Li/TiO_2	400	92		8 (3)	
	600	1.7	95 (2)		2.8 (2)
Rb/TiO_2	400	94 (5)		6 (3)	
	600	99 (2)	0.6 (3)		

concentration of the samples are shown in Table 2 and the XRD patterns in Figs. 2 and 3. On samples with lithium, the substitution of this atom for titanium in the polymorphic TiO_2 phases was not likely

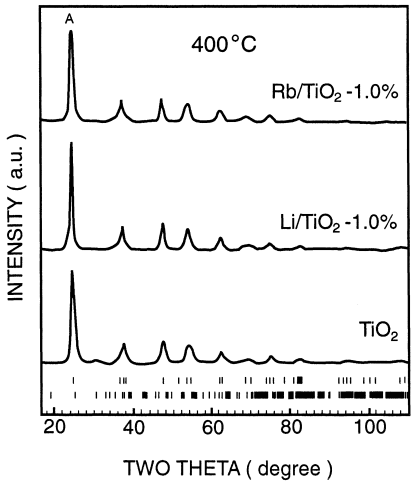

Fig. 2. Rietveld refinements plots for TiO_2, Li/TiO_2 and Rb/TiO_2 sol–gel catalysts annealed at 400°C. Upper tick marks correspond to anatase phase and lower tick marks to brookite phase.

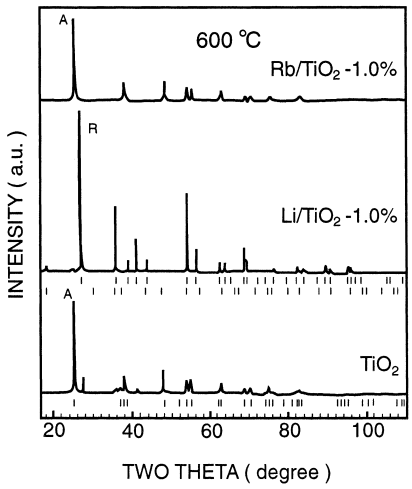

Fig. 3. Rietveld refinements plots for TiO_2, Li/TiO_2 and Rb/TiO_2 sol–gel catalysts annealed at 600°C. Upper tick marks correspond to rutile phase and lower tick marks to anatase phase.

because of its small size. On the other hand rubidium substitution for titanium was considered in the data.

Samples annealed at 400°C showed a crystalline structure similar to anatase with small contribution of brookite structure. The small brookite concentration showed a random variation also small for pure and doped samples. Then, anatase phase was stable for all samples until 400°C. At 600°C anatase was partially transformed to rutile phase in pure titania.

In lithium doped sample, annealed at 600°C, most of the anatase phase was transformed into rutile with an additional formation of the lithium–titanium compound $LiTi_2O_4$ in a small concentration. This means that anatase was transformed into rutile for temperatures higher than 600°C and some lithium reacts with TiO_2.

In rubidium doped samples the anatase structure was preserved until 600°C. At this temperature, brookite disappeared and the sample was constituted by single anatase structure with a very small concentration of rutile. Table 3, shows the average crystallite size as a function of temperature and dopant concentration. Crystallite size increases with the temperature but it is kept into the nanocrystalline regime. Rutile crystallite size was lightly larger than for anatase. Comparison of results for doped samples with each other and with pure TiO_2 samples allows us to speculate that substitution of lithium or rubidium for titanium by means of the sol–gel technique is a promising procedure to stabilize nanocrystalline titania phases.

Table 3
Titania phase average crystallite size as a function of dopant and temperature

Catalyst	(°C)	Anatase (nm)	Rutile (nm)	Brookite (nm)	$LiTi_2O_4$ (nm)
TiO_2	400	13.8 (7)		26 (51)	
	600	43 (1)	65 (23)		
Li/TiO_2	400	17.0 (8)		13 (6)	
	600	78 (52)	127 (4)		78 (47)
Rb/TiO_2	400	14.6		12 (13)	
	600	38 (1)	60 (36)		

3.4. Catalytic activity

The activities of the samples were determined in the 2,4-dinitroaniline decomposition at room temperature. The decomposition of the reactant was followed by the UV absorption band at 346 nm. The evolution of the 2,4-dinitroaniline as a function of time is represented in Fig. 4. In samples annealed at 400°C the evolution of reactant decomposed in function of the time is shown in Fig. 5. For a correct evaluation of the data, we applied the Langmuir–Hinselwood model using the equation for heterogeneous photocatalytic reactions [5]:

$$r = \frac{k_1 k_2 C}{1 + k_2 C}$$

This equation became linear as:

$$\frac{1}{r} = \frac{1}{k_1} + \frac{1}{k_1 k_2 C}$$

For a batch reactor we have:

$$-\frac{V\,\mathrm{d}C}{\mathrm{d}t} = \frac{mAk_1k_2C}{1 + k_2C}$$

integrating from $t = 0$ to $t = i$ and for the initial concentration C_0 to the C_i concentration, we have:

$$\left(\frac{\ln C_0/C}{C_0 - C}\right) = -\frac{k_2 + (mAk_1k_2)t}{(V(C_0 - C))}$$

and finally to estimate the time in which $C_0 = C_0/2$ we use:

$$t_{1/2} = \frac{[(0.693/k_1k_2) + (C_0/2k_1)]}{(mA/V)}$$

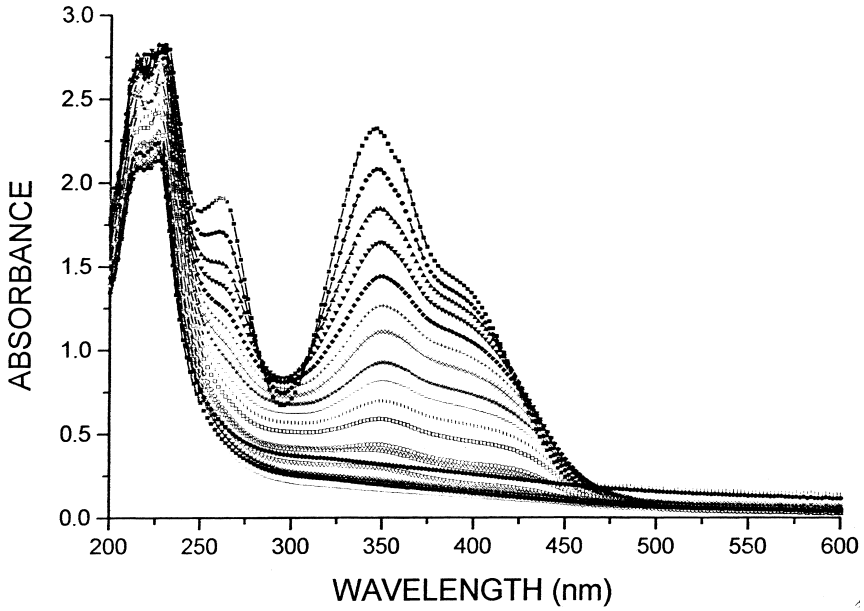

Fig. 4. UV–VIS spectra of the evolution of the 346 nm absorption band for the 2,4-dinitroaniline decomposition.

where r is the reaction rate, k_1 the apparent rate constant, k_2 the adsorption constant, m the mass of catalyst, A the adsorption sites by g/cat, V the liquid volume.

The values of $t_{1/2}$ were estimated from the data illustrated in Fig. 6 and they are tabulated in Table 4.

The activities expressed as $t_{1/2}$ for TiO_2 and Li/TiO_2 show that in general in the latter the activity is lower. It is noticeable that in samples annealed at 400°C the anatase and brookite phases are present in comparable amounts for both catalysts, however, the activity is quite different. Moreover the E_g for both catalysts

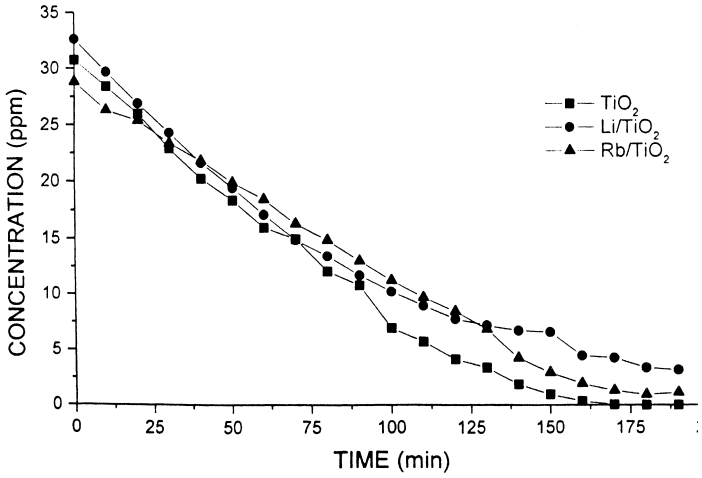

Fig. 5. Evolution on function of time for the photodecomposition of the 2,4-dinitroaniline on TiO_2, Li/TiO_2 and Rb/TiO_2 sol–gel catalysts annealed at 400°C.

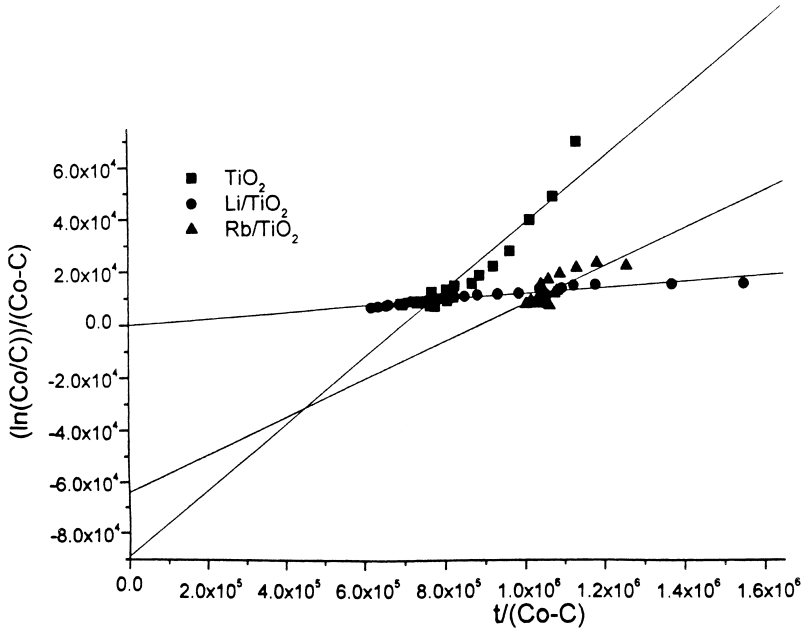

Fig. 6. Langmuir–Hinshelwood model for heterogeneous photocatalytic reactions in the 2,4-dinitroaniline decomposition on TiO_2, Li/TiO_2 and Rb/TiO_2 sol–gel catalysts annealed at 400°C.

have values of the same order, 3.27 and 3.32 eV, respectively. For the samples annealed at 600°C, the main phase is anatase for TiO_2 and rutile for Li/TiO_2 and the activities were 13.4 and 57.2 min, respectively. Such results induce us to propose, that the effect of Li in TiO_2 prepared by sol–gel (addition of lithium precursor in the gel) is mainly an effect due to its incorporation in the TiO_2 network. Its role is limited to inhibiting the reaction rate by trapping the electrons or the holes produced during the UV radiation. Lithium could be present as interstitial Li^0, since it has been reported that dehydroxylation has an important reducing role [21,22]. On the other hand, lithium could also be present as Li–O substituting Ti^{4+} because of its small ionic radius (0.60 Å), which is comparable to that of Ti^{4+} (0.68 Å). Then an inhibition of the oxidation reaction will occur in spite of the fact that the physical chemistry properties (E_g and titania crystalline phases mainly) apparently are not modified.

Table 4
Results of the Langmuir–Hinshelwood model for the 2,4-dinitroamiline decomposition on TiO_2, Li/TiO_2 and Rb/TiO_2 sol–gel catalysts

Catalyst	(°C)	$k_1(10^6)$	k_2	k_1k_2	$t_{1/2}$ (min)
TiO_2	400	3.6	88830	0.317	5.5
	600	3.0	42625	0.130	13.4
Li/TiO_2	400	13.0	2871	0.037	46.9
	600	8.6	3834	0.033	57.2
Rb/TiO_2	400	2.1	63142	0.177	9.8
	600	4.6	20969	0.090	17.8

In rubidium-doped titania compared with TiO_2 the activities for the samples annealed at 400°C, are of the same order ($t_{1/2}$ of 9.8 and 5.5 min, respectively). Note that the crystalline phase composition showed for the samples (94% anatase and 6% brookite) is similar and the same is observed in the E_g values, 3.27 eV for both samples. In this case we can assume that the Rb insertion in the titania network is in a smaller amount than those presumed for lithium. We can expect that rubidium could be present as trapped Rb_2O in titania as well as Rb_2O highly dispersed on the titania surface. Because of its ionic radius (1.48 Å), the Rb must migrate to the titania surface as the annealing temperature is increased. At 600°C the Rb_2O on the surface will be present in a large amount and then its role in the activity is negligible, the $t_{1/2}$ value for TiO_2 is 13.4 min and that of rubidium doped titania is 17.8 min.

4. Conclusions

The preparation of TiO_2 and Li and Rb doped titania by the sol–gel method produce samples showing specific surface areas between 111 and 89 m^2/g, when they are annealed at temperatures of 400°C. By increasing the temperature the specific surface areas are notably diminished as usually observed in titania.

The E_g values obtained for the various samples, doped and un-doped, are between the reported values for anatase and rutile or for the mixture of both phases. Such results indicate that the doping of titania with Li and Rb has little effect on the band gap when comparing with the reference preparation.

The crystalline phase composition determined by X-ray diffraction, showed the expected evolution from anatase to rutile as a function of the annealing temperature for the TiO_2. However, in Li/TiO_2 the formation of $LiTi_2O_4$ compound is observed at high temperatures. In the case of Rb/TiO_2 the stabilizing effect of Rb for the anatase phase is observed. In all cases the preparation method proved to be one by which nanocrystalline structures can be obtained.

When the samples were tested in the 2,4-dinitroaniline decomposition, an inhibiting effect of the activity is obtained in lithium doped samples, while in Rb doped ones no considerable effect is observed. It was proposed that a large percentage of Li could be trapped in the titania network playing the role of electron trapping when it is as Li–O or hole trapping ones when it is present as Li^0. On the other hand, because of its ionic radius Rb preferentially migrates to the titania surface, must probably forming largely Rb_2O clusters on the surface, the residual Rb_2O remaining in the TiO_2 network play a role limited to stabilize the anatase phase, since its activities were comparable to the TiO_2 reference catalyst.

The main conclusion is then, when titania is doped with alkaline metals the effects in activity can only be observed if the ionic radius of the metal is equal or smaller than that of Ti^{4+} ionic radius. Moreover, the metal must be inserted in the titania network, otherwise, no effect is produced.

Acknowledgements

We are indebted to CONACYT for financial support.

References

[1] I. Arslan, I.A. Balcioglu, D.W. Bahnemann, Appl. Catal. B Environ. 26 (2000) 193.
[2] Q. Zhang, L. Gato, J. Guo, Appl. Catal. B Environ. 26 (2000) 207.
[3] J. Taguchi, T. Okura, Appl. Catal. A Gen. 194/195 (2000) 89.
[4] M.I. Litter, Appl. Catal. B Environ. 23 (1999) 89.
[5] N. Serpone, E. Pelizzetti, Photocatalysis Fundamental and Applications, Wiley, New York, 1989.
[6] Y. Xu, Z. Zhu, W. Chen, G. Ma, Chin. J. Appl. Chem. 8 (1991) 28.
[7] M. Ampo, T. Shima, S. Kodama, Y. Kubokawa, J. Phys. Chem. 91 (1987) 4305.
[8] L. Pauling, J. Am. Chem. Soc. 51 (1929) 1010.
[9] X. Bokhimi, A. Morales, O. Novaro, T. López, E. Sánchez, R. Gómez, J. Mater. Res. 10 (1995) 2788.
[10] T. López, R. Gómez, J.L. Boldu, E. Muñoz, X. Bokhimi, O. Novaro, Mat. Res. Soc. Symp. Proc. 380 (1995) 81.
[11] T. López, E. Sánchez, React. Kinet. Catal. Lett. 48 (1992) 295.
[12] T. López, E. Sánchez, P. Bosch, Y. Meas, R. Gómez, Mater. Chem. Phys. 32 (1992) 141.
[13] E. Sánchez, T. López, Mater. Lett. 25 (1995) 271.
[14] T. López, E. Sánchez, R. Gómez, L. Ioffe, Y. Borodko, React. Kinet. Catal. Lett. 61 (1997) 289.
[15] E. Sánchez, T. López, R. Gómez, X. Bokhimi, A. Morales, O. Novaro, J. Solid State Chem. 122 (1996) 309.
[16] R. Gómez, T. López, S. Castillo, R.D. Gonzalez, J. Sol–Gel Sci. Tecnol. 1 (1994) 205.
[17] R.A. Young, R. Von Dreele, Rietveld Method Short Course, Continuing Education, Georgia Institute of Technology, 1993.
[18] International Tables for X-ray Crystallography, Vol. IV, Kynoch Press, Birmingham, UK, 1974.
[19] P. Thompson, D.E. Cox, J.B. Hastings, J. Appl. Crystallogr. 20 (1987) 79.
[20] L.A. Grumes, R.D. Leapman, C.N. Wilker, R. Hoffmann, A.B. Kuns, Phys. Rev. B 25 (1982) 7157.
[21] T. López, R. Gómez, in: L.C. Klein (Ed.), Sol–Gel Optics Processing and Applications, Kluwer Academic Publishers, Dordrecht, 1994, Chapter 16, p 345.
[22] X. Bokhimi, O. Novaro, R.D. Gonzalez, T. López, O. Chimal, A. Asomoza, R. Gómez, J. Solid State Chem. 144 (1999) 349.